



Imaging opportunities at 50-100 keV

Marco Stampanoni :: Head of SLS-TOMCAT
Other Science Opportunities @ FCCee – CERN, November 28th 2024

Medical... vs... synchrotron X-ray imaging



First X-ray (1896)



State-of-the-art X-ray imaging in hospitals

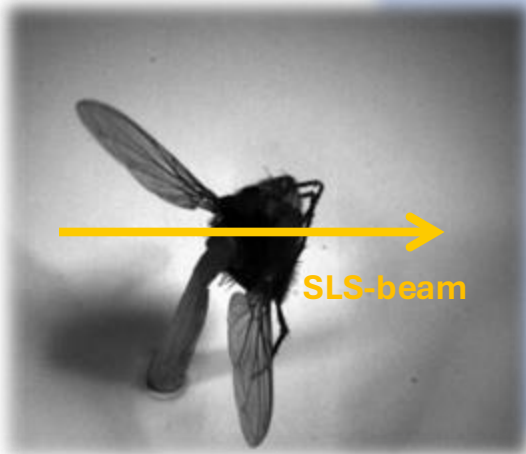


X-ray microradiography at SLS

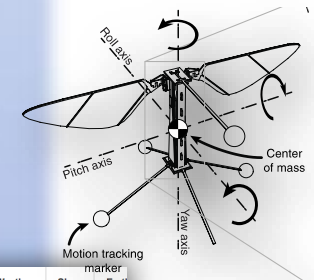
Muscles and tracheal network *during* flight



Jafferis et al., Nature 2019

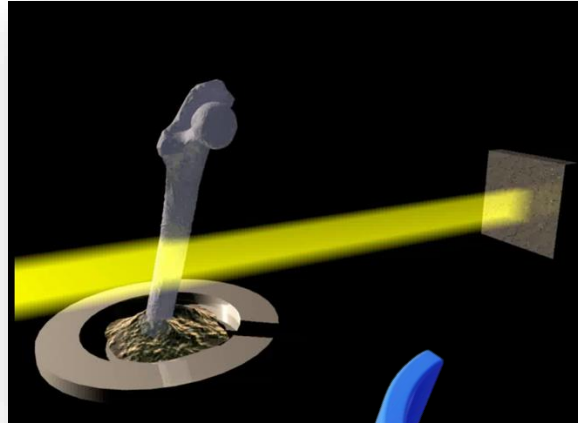


Walker et al., PloS Biology (2014) & Mokso et al., SciRep (2015)

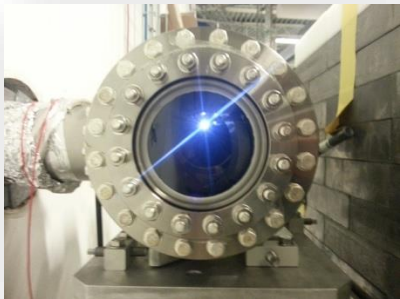
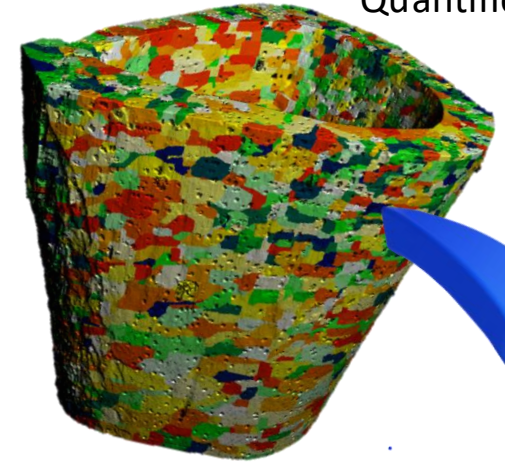


Computed tomography to gather 3D structural information from opaque samples

Measurement



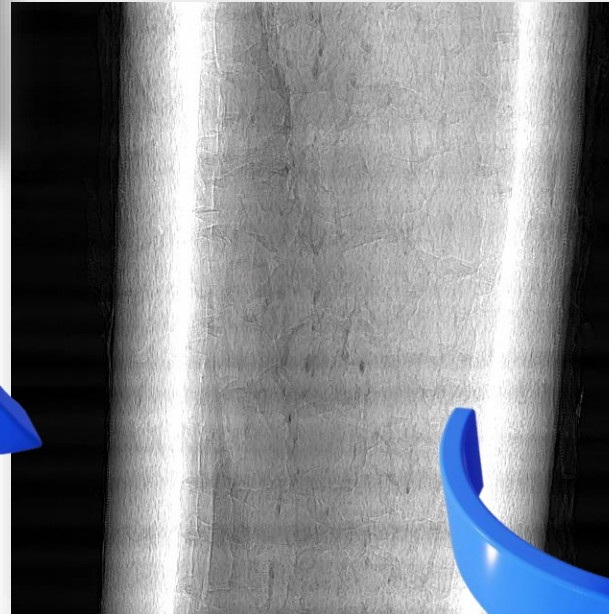
Quantification



Bright beam from the synchrotron

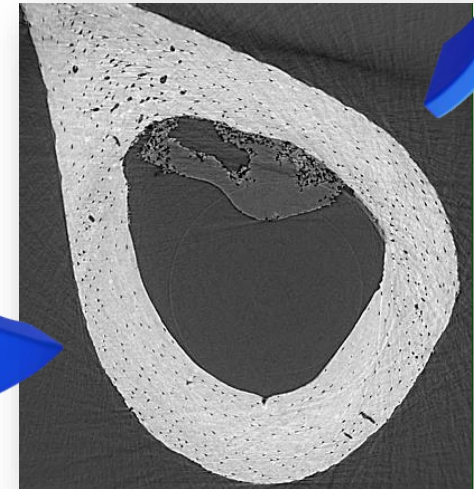
Projections $[0, \pi]$

$$P = \ln \frac{I_0}{I} = \int_0^d \mu(z) dz$$



Reconstructions

$$\mu(x, y) = \int_0^\pi d\theta \int_{-\infty}^{+\infty} \tilde{P}(\omega, \theta) |\omega| e^{j2\pi\omega t} d\omega$$



«Chasing the phase...»

General form of a wave in vacuum:

$$\psi_{vacuum}(\vec{r}, t) = Ae^{i(\vec{k}\cdot\vec{r}-\omega t)}$$

For a wave traveling in the z-direction:

$$\vec{k} = (0, 0, k = \frac{2\pi}{\lambda})$$

Plane wave propagating in z-direction:

$$\psi_{vacuum}(\vec{r}, t) = Ae^{i(\vec{k}\cdot\vec{r}-\omega t)} = Ae^{i(kz-\omega t)}$$

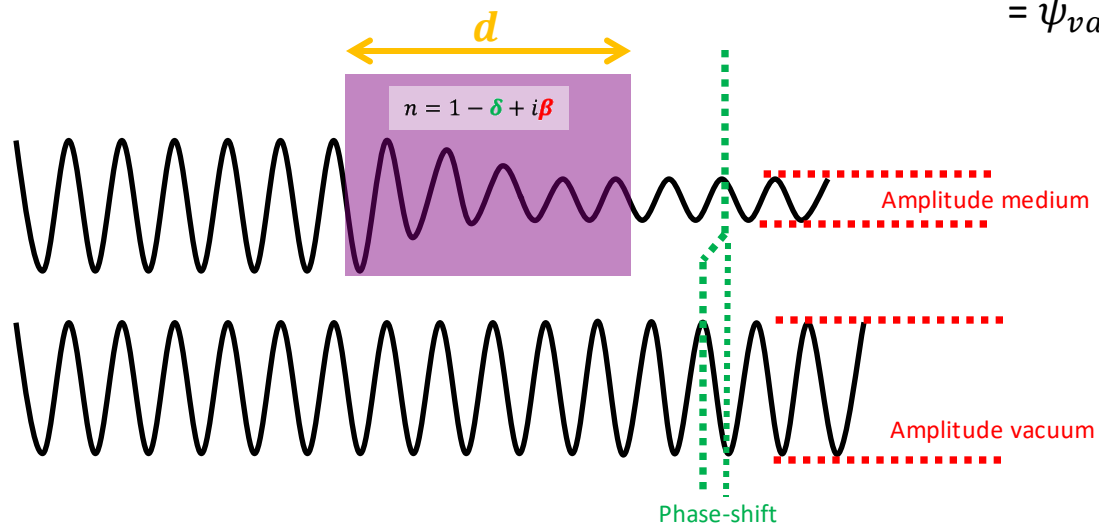
For a wave traveling in a medium:

$$n = 1 - \delta + i\beta$$

Wave propagating in a medium:

$$\psi_{medium}(z, t) = Ae^{i(nkz-\omega t)} = Ae^{-i\omega t} e^{(1-\delta)ikz} e^{-\beta kz} =$$

$$= \psi_{vacuum} \cdot \underbrace{e^{-i\delta kz}}_{\text{Phase-shift}} \cdot \underbrace{e^{-\beta kz}}_{\text{Attenuation}}$$

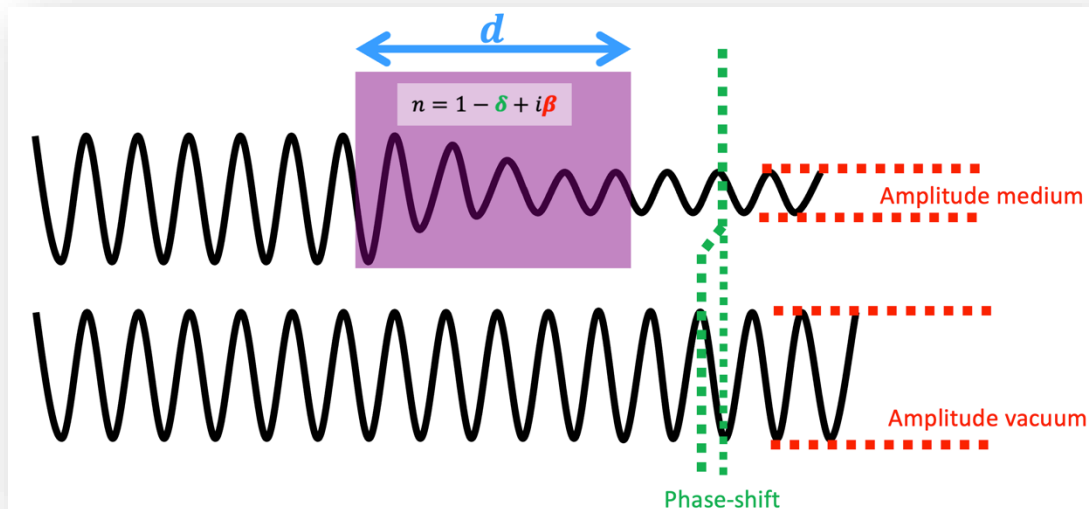


After medium of length d :

$$T(d) = \frac{I_m(d)}{I_v(0)} = \frac{|\psi_m(d, t)|^2}{|\psi_v(0, t)|^2} = e^{-2k\beta d}$$

$$\Delta\phi(d) = \delta kd$$

Why is phase interesting for imaging?



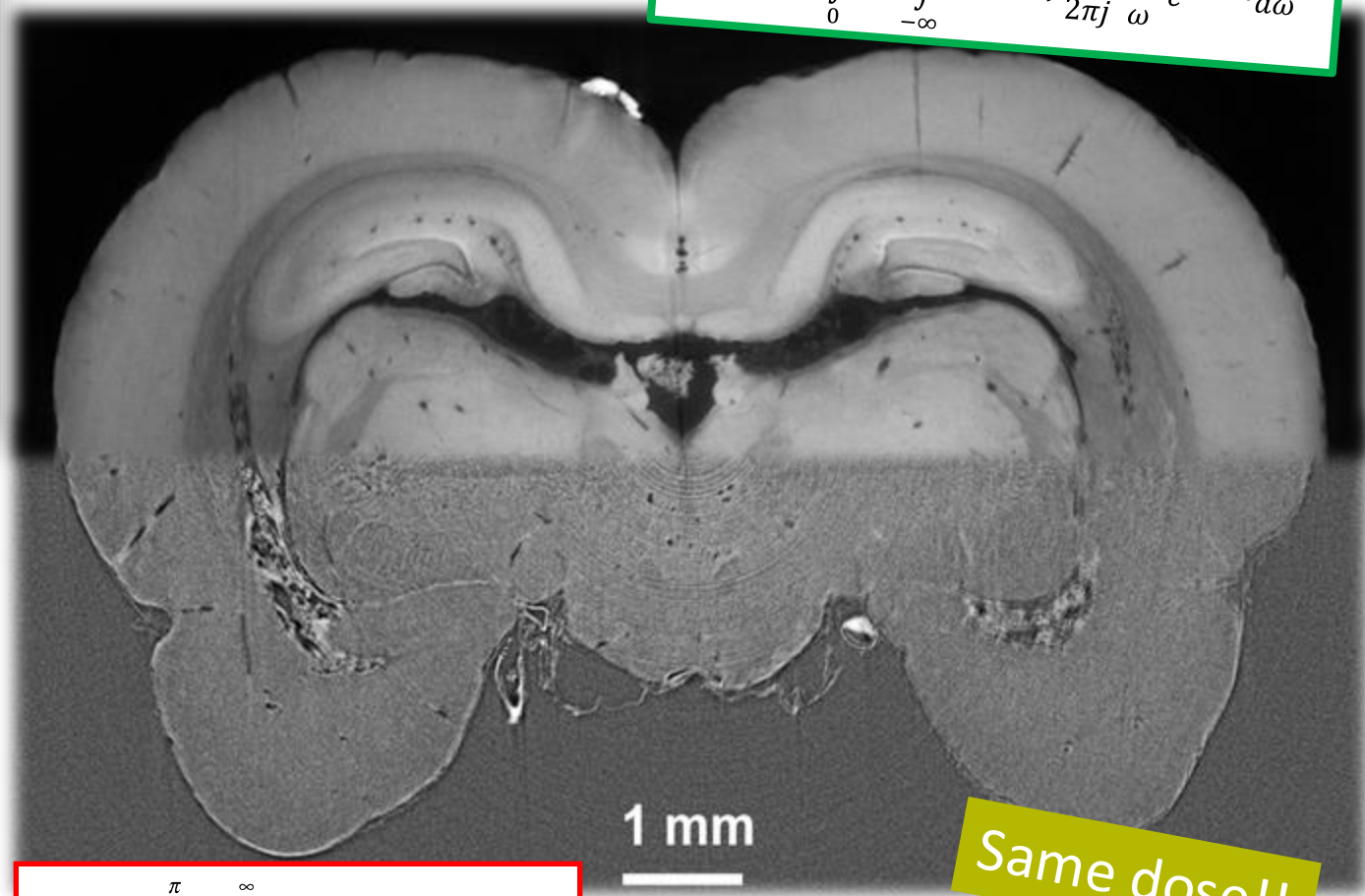
«Gedankenexperiment»

- 20 keV X-rays
- 50 μm thick organic sample

→ only 0.2 % absorption

→ but π phase shift!

} Higher contrast @ same dose

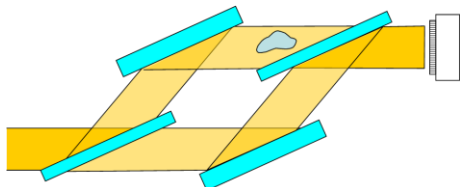


$$\delta(x, y) = \int_0^\pi d\theta \int_{-\infty}^{+\infty} \tilde{D}(\omega, \theta) \frac{1}{2\pi j} \frac{|\omega|}{\omega} e^{j2\pi\omega t} d\omega$$

$$\mu(x, y) = \int_0^\pi d\theta \int_{-\infty}^{\infty} \tilde{P}(\omega, \theta) |\omega| e^{j2\pi\omega t} d\omega$$

Accessing X-ray "phase-driven" contrast

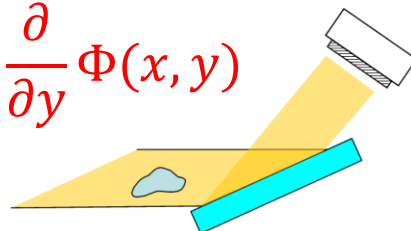
$$\Phi(x, y)$$



Crystal interferometry

Bonse et al. APL 6, 155 (1965)

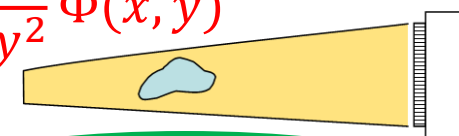
$$\frac{\partial}{\partial y} \Phi(x, y)$$



Diffraction enhanced imaging

Chapman et al., *PMB*, 42, 2015 (1997)
Davis et al., *JOSA A* 13, 1193 (1996)

$$\frac{\partial^2}{\partial y^2} \Phi(x, y)$$

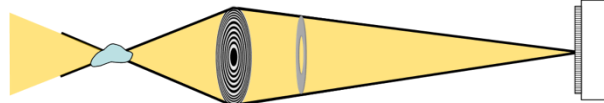


Free space propagation

Snigirev et al., *RSI* 66, 5486 (1995)
Cloetens et al., *APL* 75, 2912 (1999)

Enables ultrafast dynamic imaging!

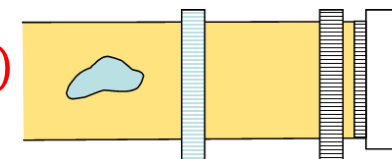
$$\Phi(x, y)$$



Zernike phase contrast

Weiss et al., *UM* 84, 185 (2000)
Holzner et al., *NatPhys* 6 (2010)

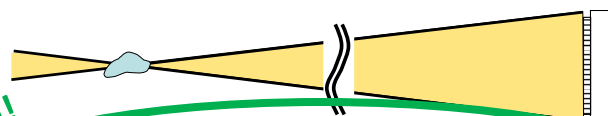
$$\frac{\partial}{\partial y} \Phi(x, y)$$



Talbot-(Lau) interferometry

Weitkamp et al., *OptExp* 13, 6296 (2005)
Pfeiffer et al., *NatPhys* 2, 258 (2006)

$$\Phi(x, y)$$



Reaches nm resolution!

Coherent diffractive imaging - Ptychography

Miao et al., *Nature* 400 (1999)
Thibault et al., *Science*, 321, 379 (2008).

Coded apertures

Olivo et al., *APL* 91 (7) 2007

Speckles

Cerbino et al., *NatPhys* 4, 2008

PHILOSOPHICAL TRANSACTIONS
OF THE ROYAL SOCIETY

On the evolution and relative merits of hard X-ray phase-contrast imaging methods

S. W. Wilkins[†], Ya. I. Nesterets, T. E. Gureyev, S. C. Mayo, A. Pogany[‡] and A. W. Stevenson

CSIRO Materials Science and Engineering, PB33, Clayton South, Victoria 3169, Australia

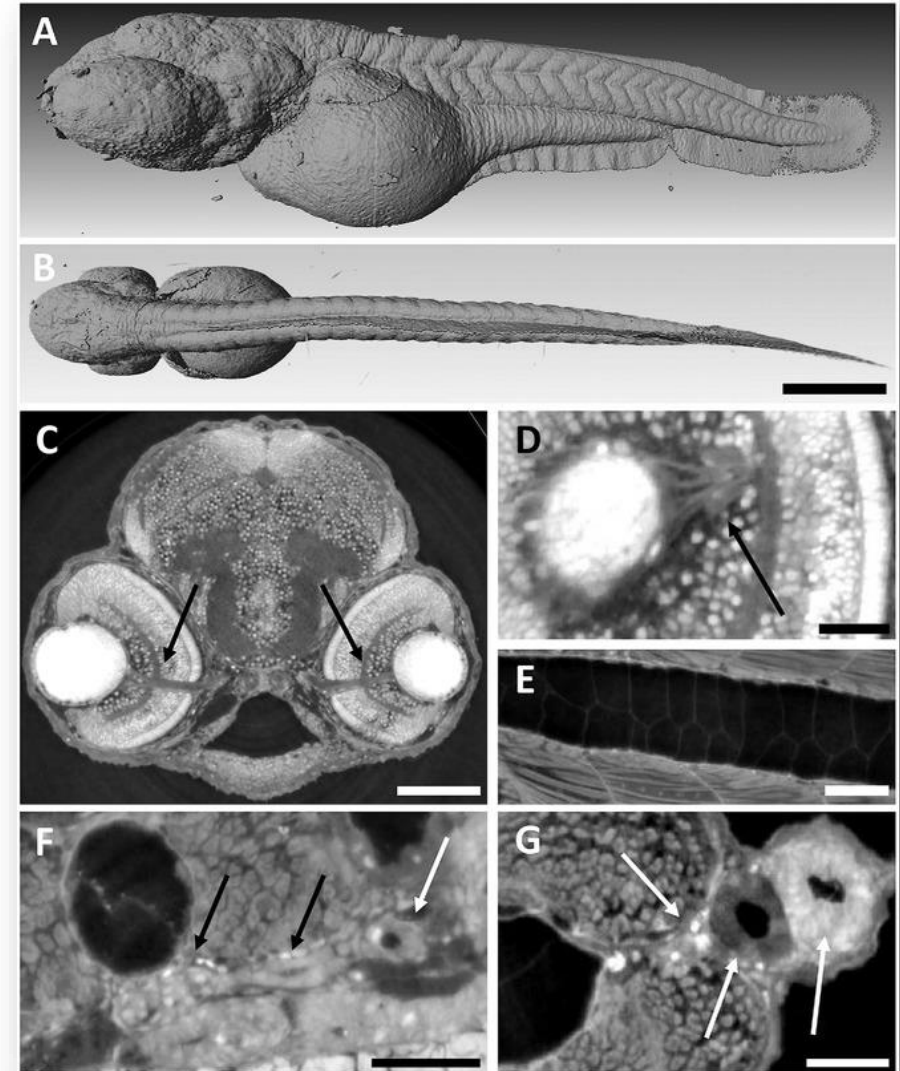
Review

CrossMark

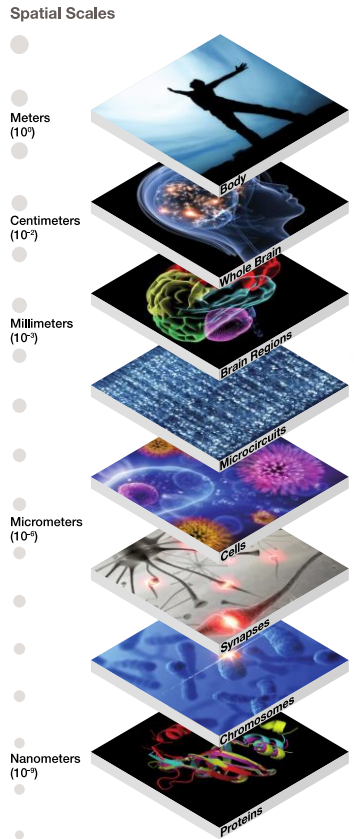
rst.a.royalsocietypublishing.org

Free-space propagation to push contrast in low-absorbing materials

$$H(\nu_x, \nu_y) = \exp \left[-i2\pi \sqrt{\frac{1}{\lambda^2} - \nu_x^2 - \nu_y^2} \cdot d \right]$$



Whole mouse brain microvascular architecture

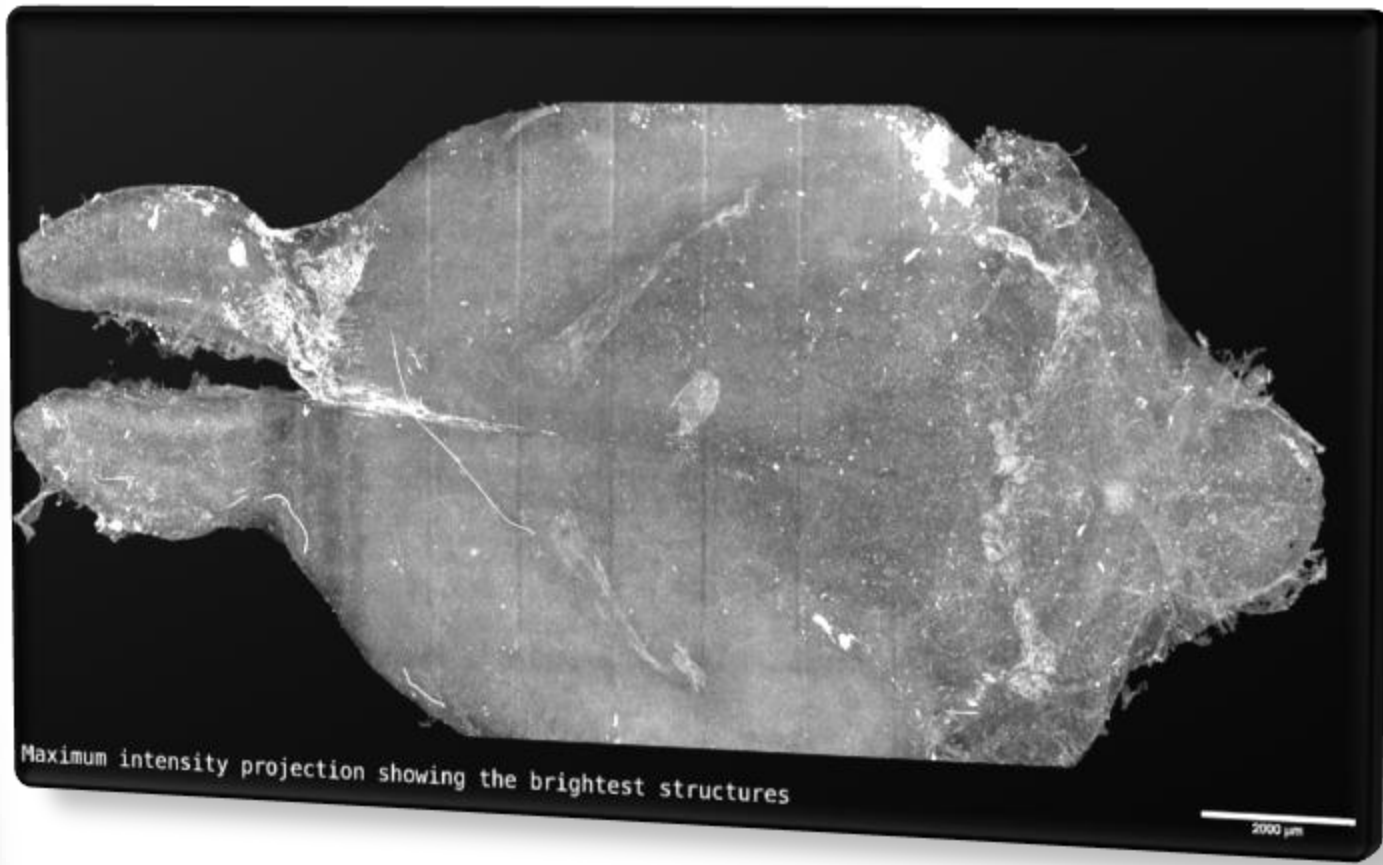


Hierarchical imaging and computational analysis of three-dimensional vascular network architecture in the entire postnatal mouse brain

Thomas Wälchli^{1,2,3,4,5}, Jeroen Bischoff^{1,2,3,4,5}, Arttu Miettinen^{6,7,8}, Alexandra Ulmer-Schuler⁹, Christoph Hintermüller¹⁰, Eric P. Meyer¹¹, Regula Wälchli¹², Philippe P. Monnier^{13,14}, Peter Carmeliet^{15,16}, Johar and Marco Stamparoni

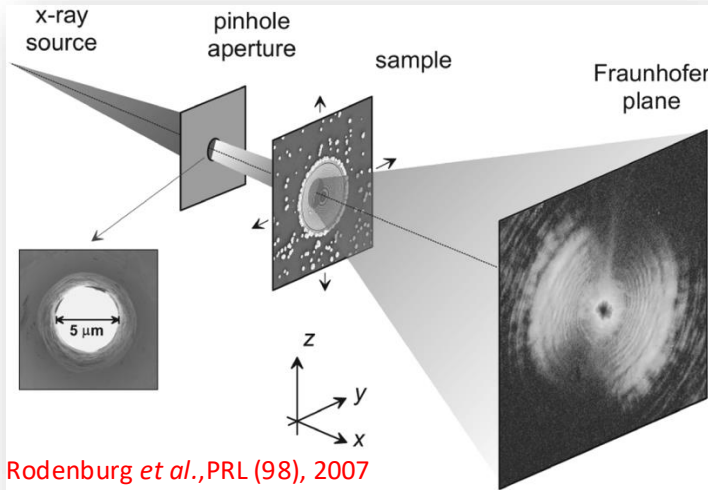
The formation of new blood vessels and the establishment of vascular networks are crucial for the adult healthy brain, as well as in various diseases of the central nervous system. We present a recently developed method that enables hierarchical imaging and computational analysis of the 3D vascular network in postnatal and adult mouse brains. The different stages of the protocol are: (1) whole brain imaging, (2) brain region segmentation, (3) microcircuit reconstruction, (4) cell reconstruction, (5) synapse reconstruction, (6) chromosome reconstruction, and (7) protein reconstruction. Combining these methods enables detailed view of brain vasculature. Network features such as vascular volume, fractal, branch order, and topological network analysis. Combining these methods enables detailed view of brain vasculature. Network features such as vascular volume, fractal, branch order, and topological network analysis. Combining these methods enables detailed view of brain vasculature. Network features such as vascular volume, fractal, branch order, and topological network analysis.

Miettinen *et al.*, Bioinformatics 2019 - Wälchli *et al.*, Nature Protocols 2022



Stitched tomogram of more than 1000 single volumes, assembled non-rigidly. Size of data shown: 12 TB

Ptychography leverages on coherence to push resolution PSI



Coherence:



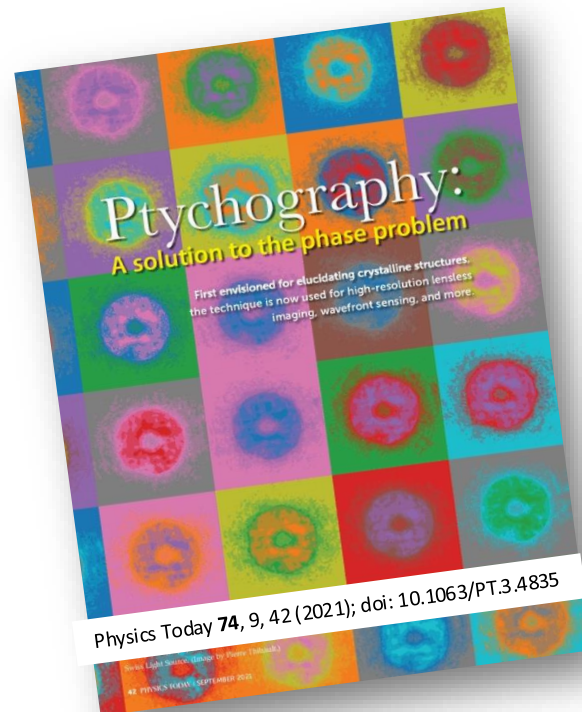
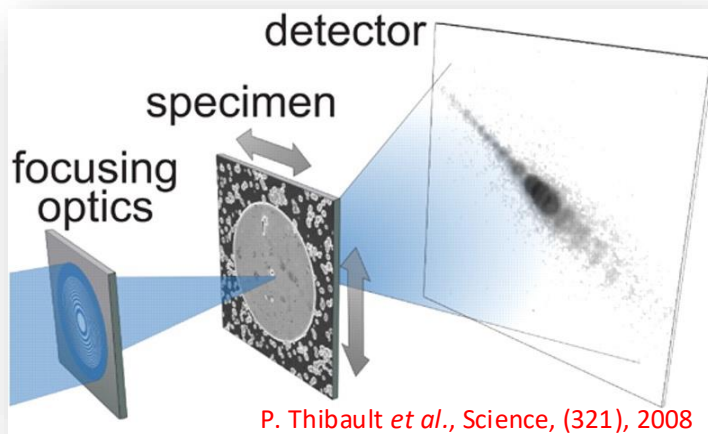
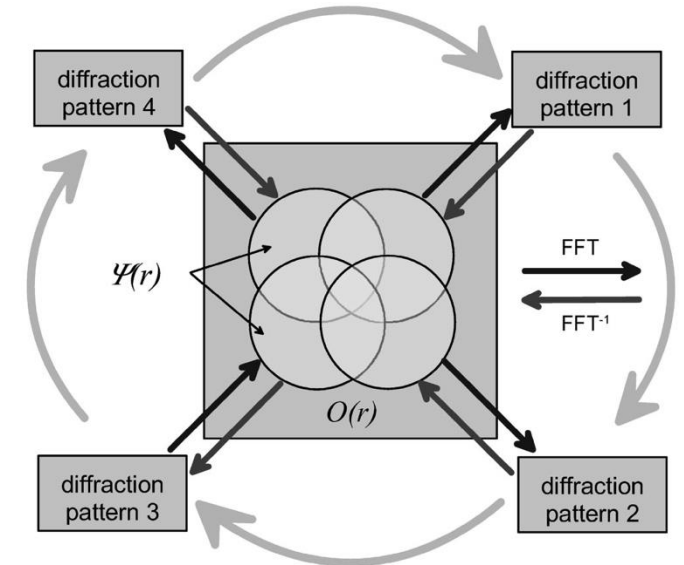
allows the interpretation of observations based on modeling of propagation and interaction with matter

Measurement:



leads to the loss of part of the information

This is the phase problem!



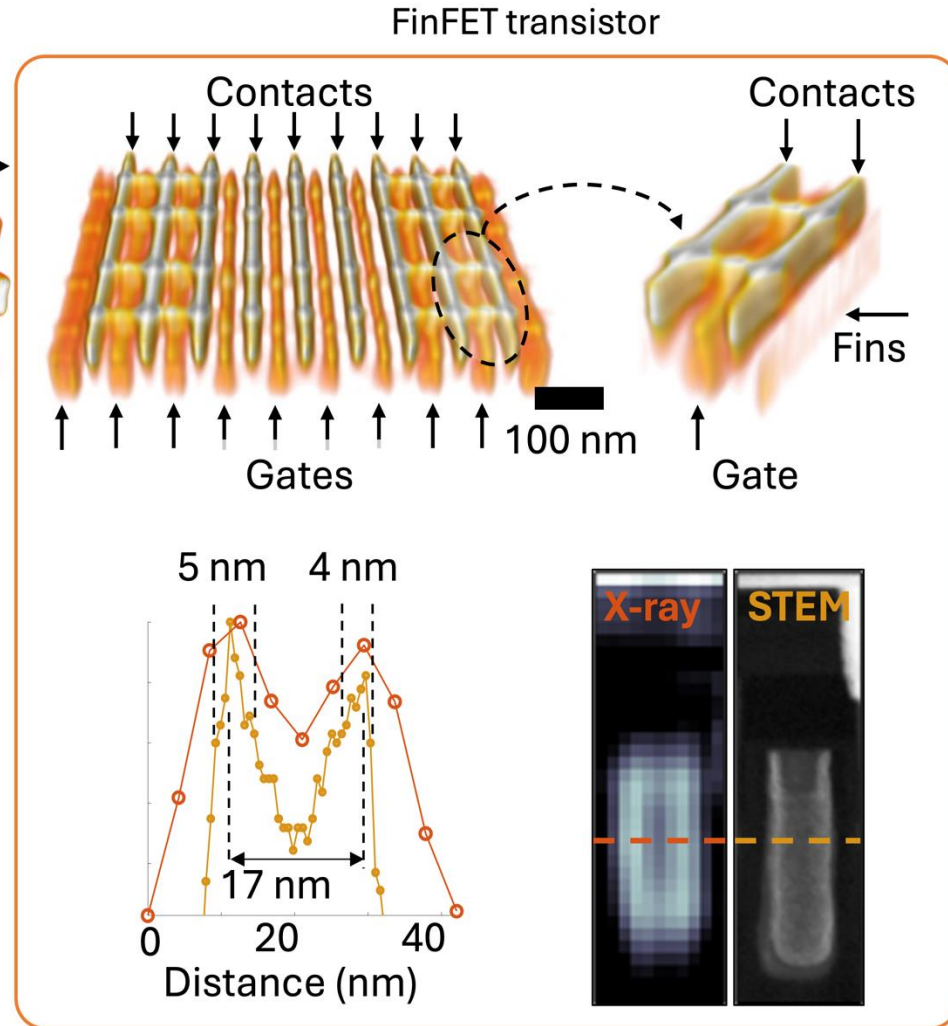
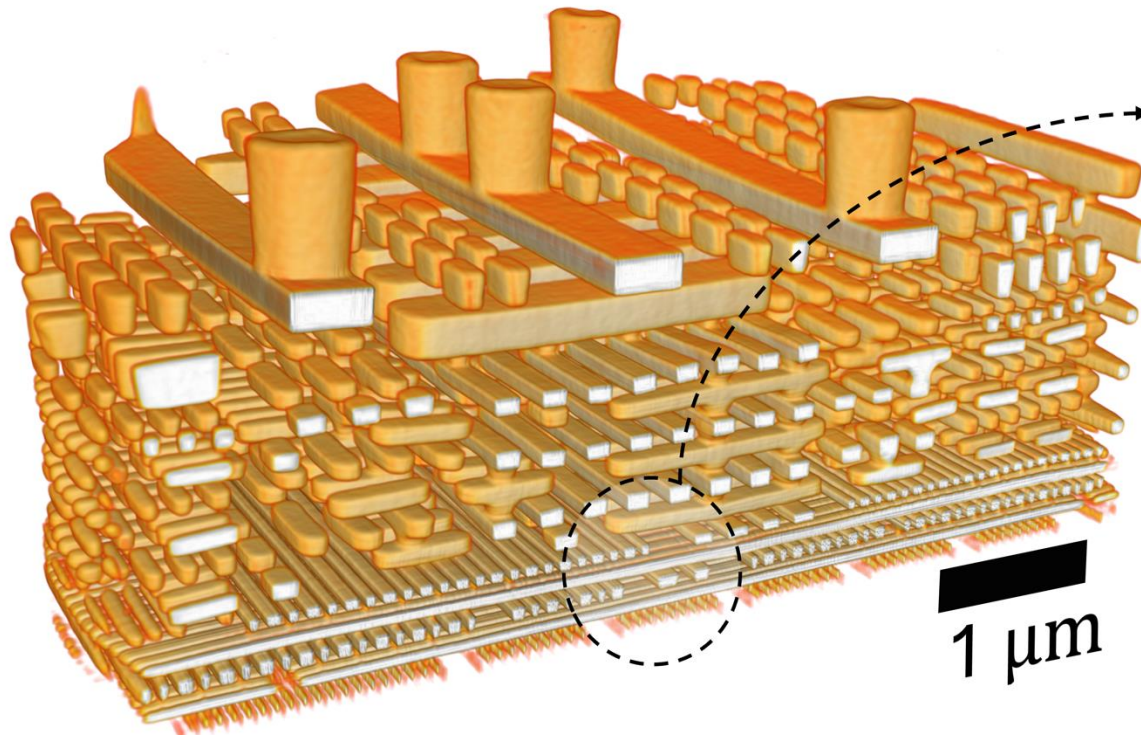
Ptychographic Iterative Engine (PIE)

- Initial exit wave calculation (based on current estimate)
- Propagation to the Fraunhofer plane
- Modulus replaced by recorded data while preserving phase (usual for iterative methods)
- Back-propagation
- Resulting difference used to update the estimate

Important note: subsequent data from adjoining areas are fed into the algorithm to speed up convergence!

Burst ptychography yields to **4 nm** resolution tomogram

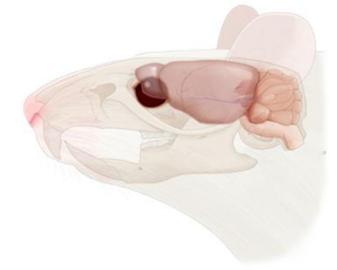
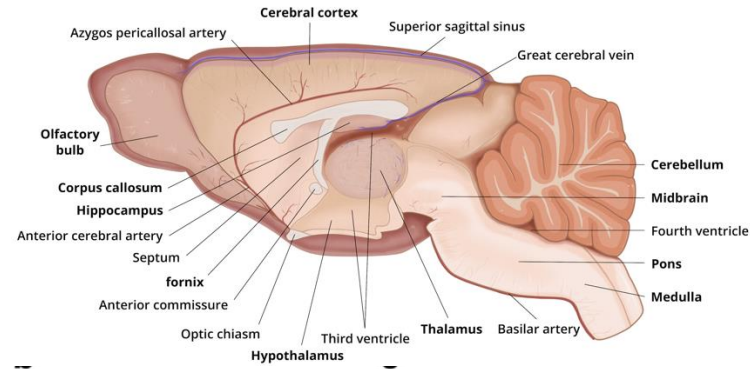
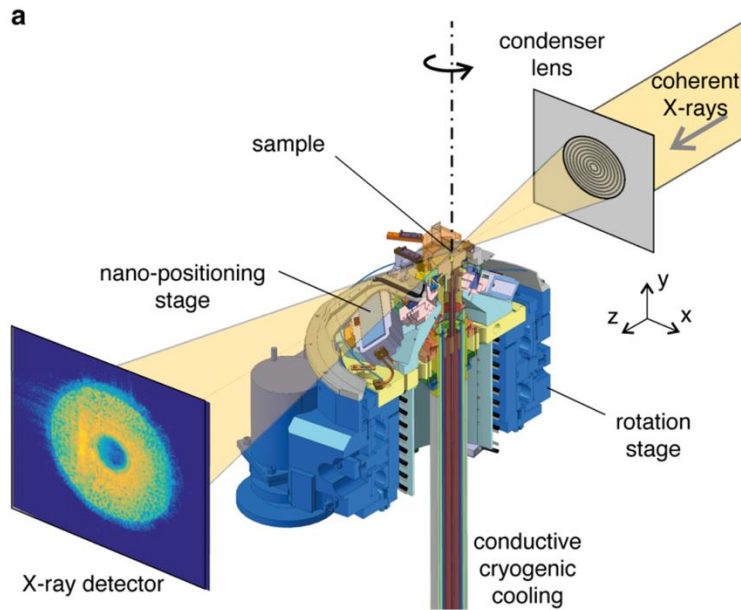
Highest X-ray tomography resolution to date!



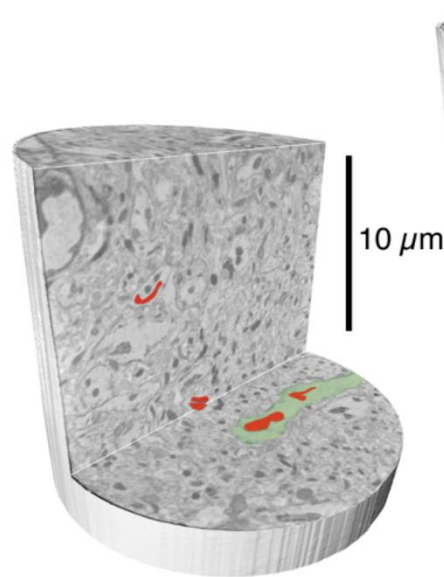
Aidukas, T., Phillips, N.W., Diaz, A. et al. High-performance 4-nm-resolution X-ray tomography using burst ptychography. Nature 632, 81–88 (2024). <https://doi.org/10.1038/s41586-024-07615-6>



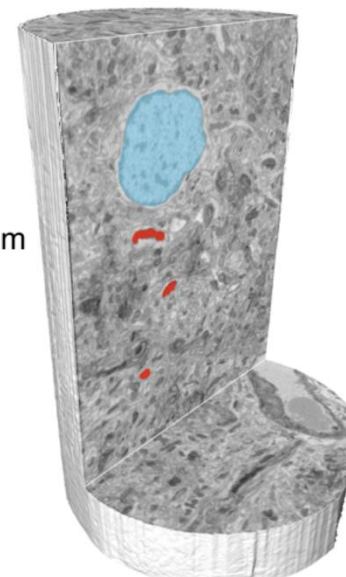
Towards synaptic mapping (connectome)



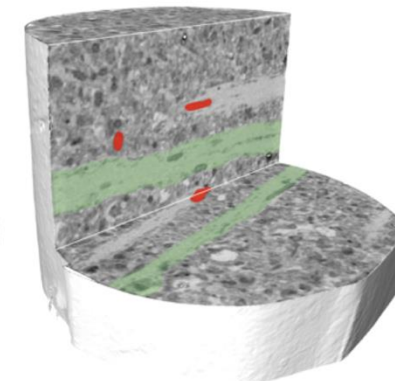
a



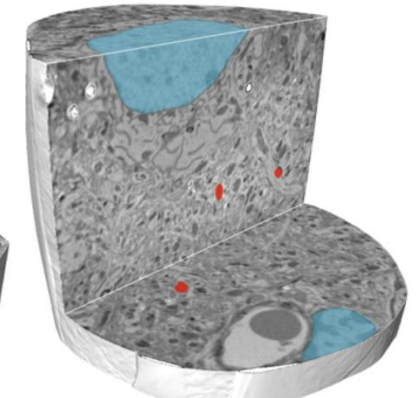
olfactory bulb
external plexiform layer



olfactory bulb
glomerular layer



hippocampus
stratum radiatum

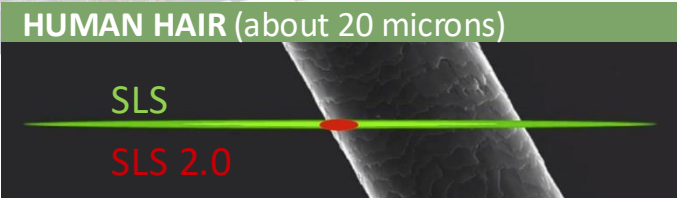
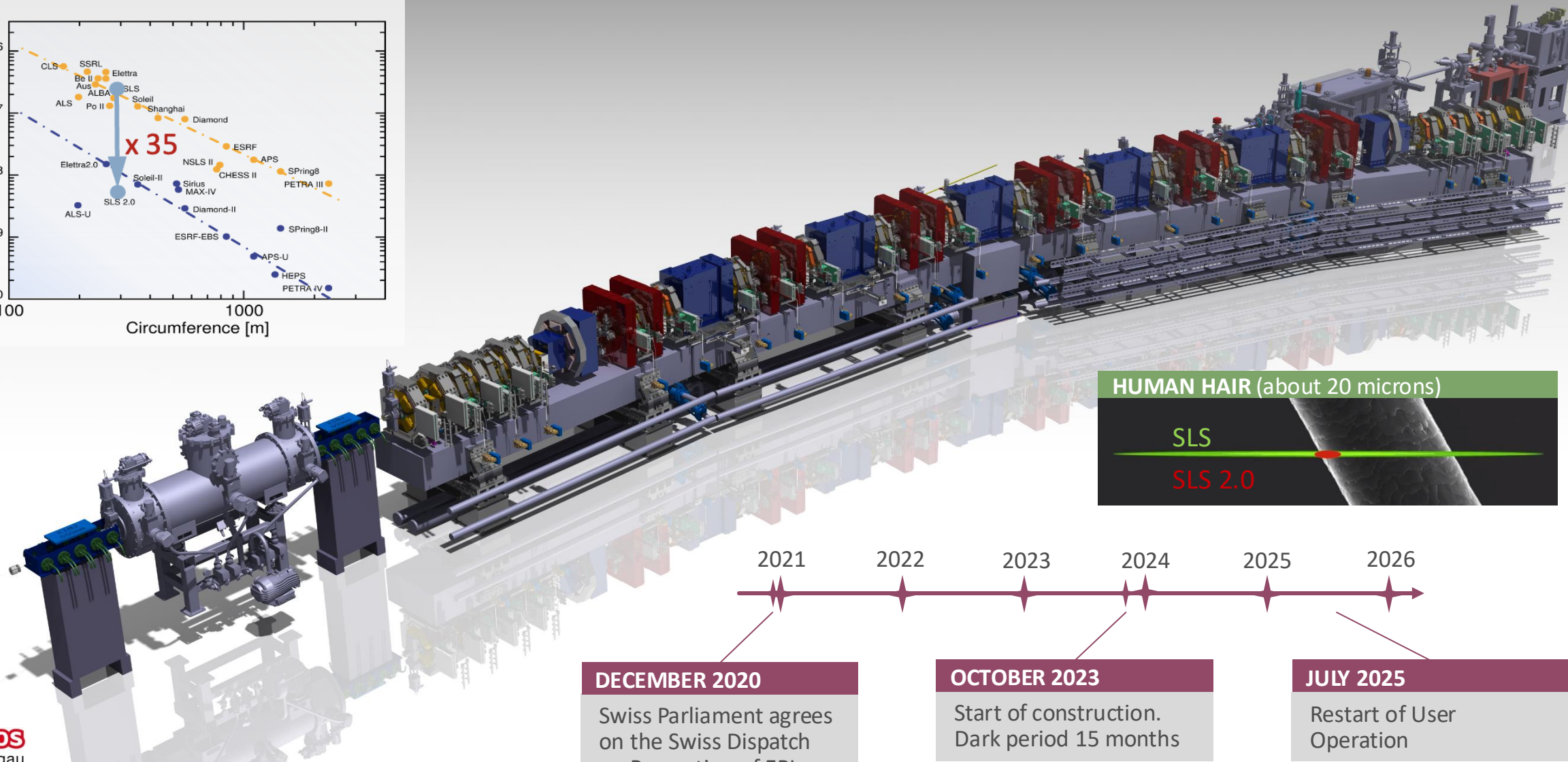
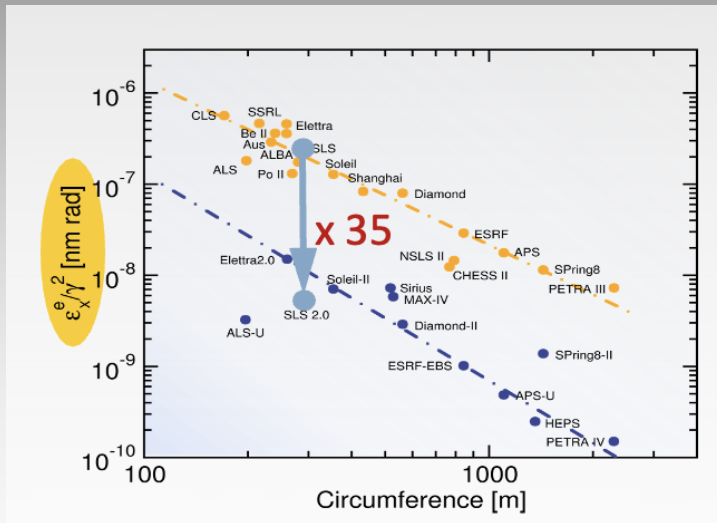


somatosensory cortex
layer 2-3

d

Bosch et al. <https://doi.org/10.1101/2023.11.16.567403> (bioRxiv)

SLS 2.0: sharper and faster imaging



DECEMBER 2020
Swiss Parliament agrees on the Swiss Dispatch on Promotion of ERI

OCTOBER 2023
Start of construction.
Dark period 15 months

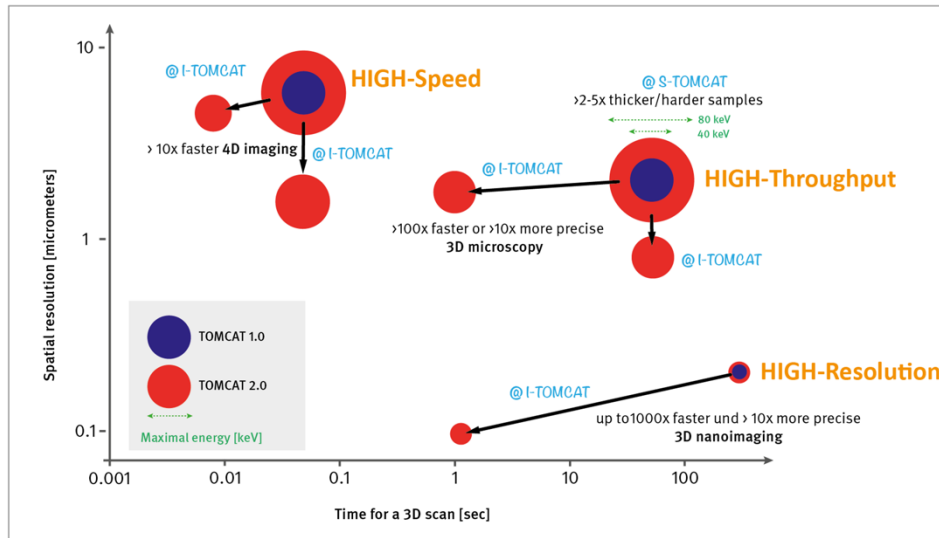
JULY 2025
Restart of User Operation

Push imaging on SLS2.0

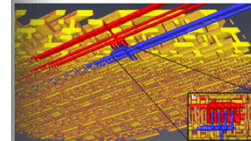
TOMCAT2.0 and cSAXS upgrade programs

TOMCAT2.0 → I-TOMCAT and S-TOMCAT

In a nutshell: Multiscale – Multimodal – Dynamic



X-ray ptychography at cSAXS at SLS 2.0



M. Holler *et al.*,
Nature **543**, 402 (2017)

Calculations from one of our measurements in 2017 at 6.2 keV, called here “state of the art”

DEVELOPMENT	RESOLUTION (nm)	VOLUME (μm^3)	TIME
State of the art	14.6	15x15x8	22 h
SLS-2 (x30)	6.4	82x82x8	44 min
+ new undulator(x2)	5.5	116x116x8	22 min

Numbers indicate the gain in one parameter with respect to the **state of the art** (M. Holler *et al.*, 2017) when keeping the other two parameters constant

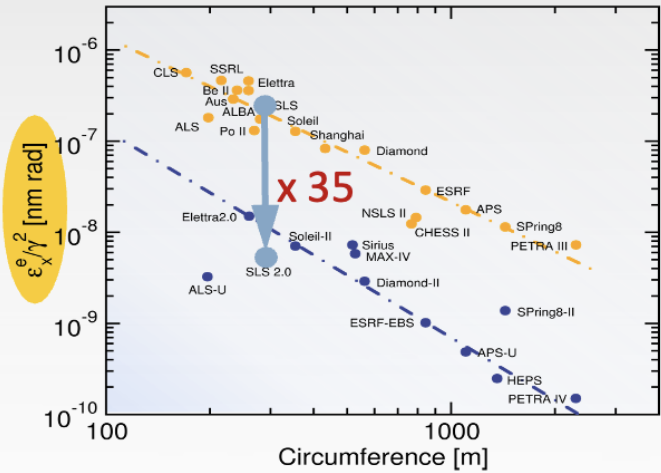
On SLS2.0 we can expect

- 2.5x better resolution at same volume and acquisition time compared to SLS1.
- 60x larger volume at same resolution and acquisition time compared to SLS1
- 60x faster for same resolution and volume compared to SLS1

“Caveat”: how much dose/flux will a sample at the end tolerate?

This might be efficiently mitigated if dose can be traded in with measurement at high-energies!

SLS 2.0: sharper and faster imaging

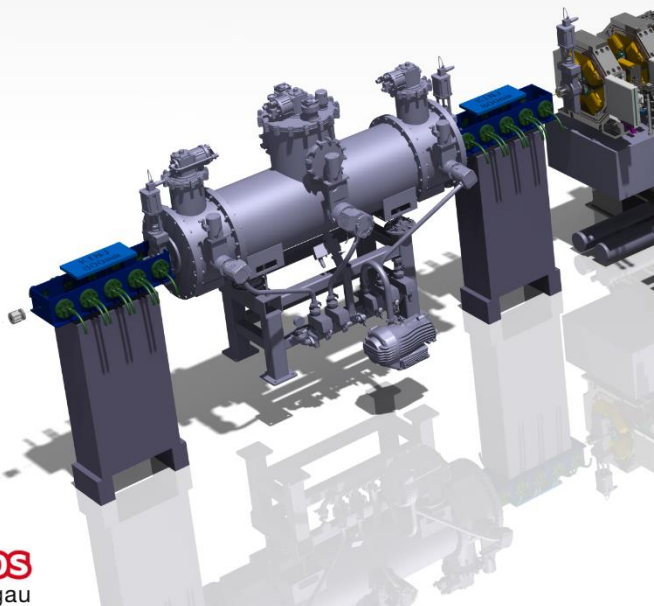
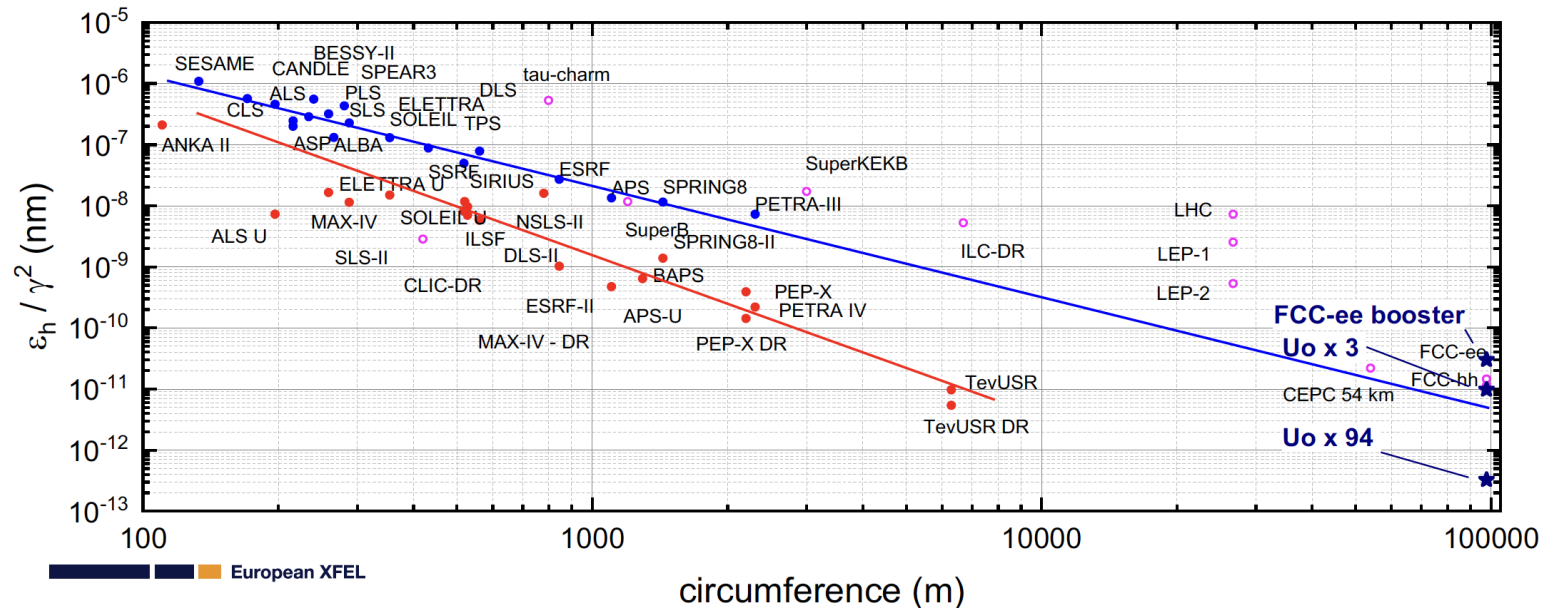


FCC-ee booster as a Light Source

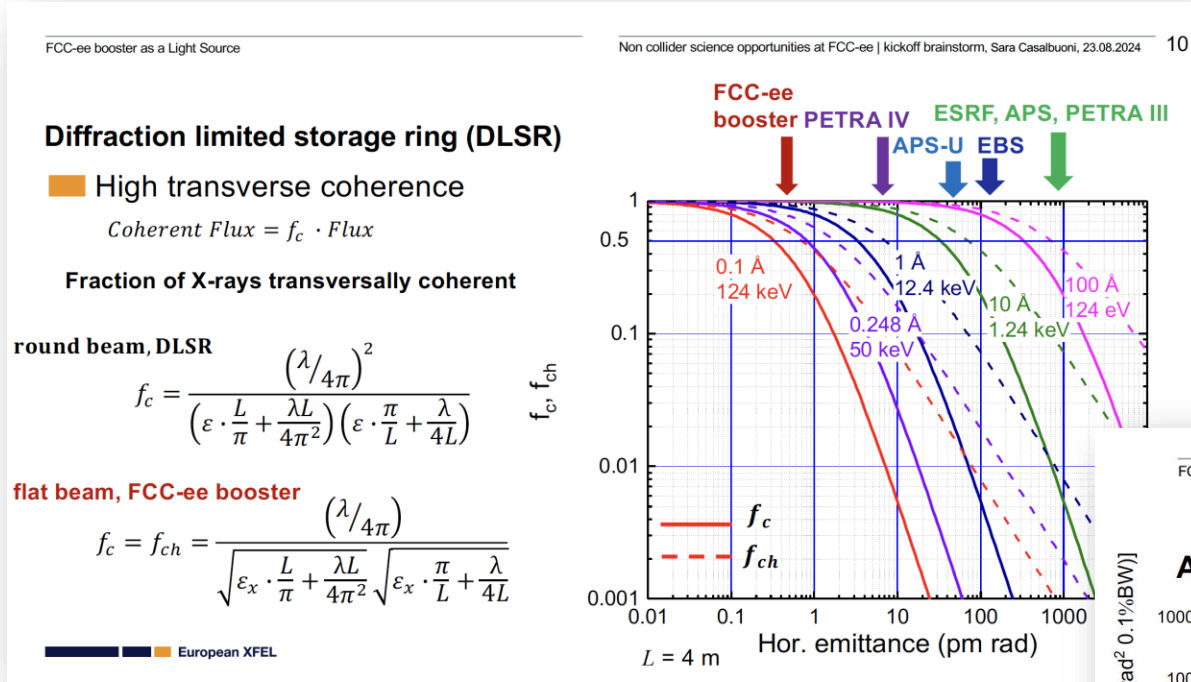
Non collider science opportunities at FCC-ee | kickoff brainstorm, Sara Casalbuoni, 23.08.2024

Horizontal emittance versus circumference

- Storage ring photon sources upgrades to decrease the horizontal emittance
- FCC-ee booster small emittance as a result of large circumference + damping wigglers/undulators



Imaging on FCC-ee?



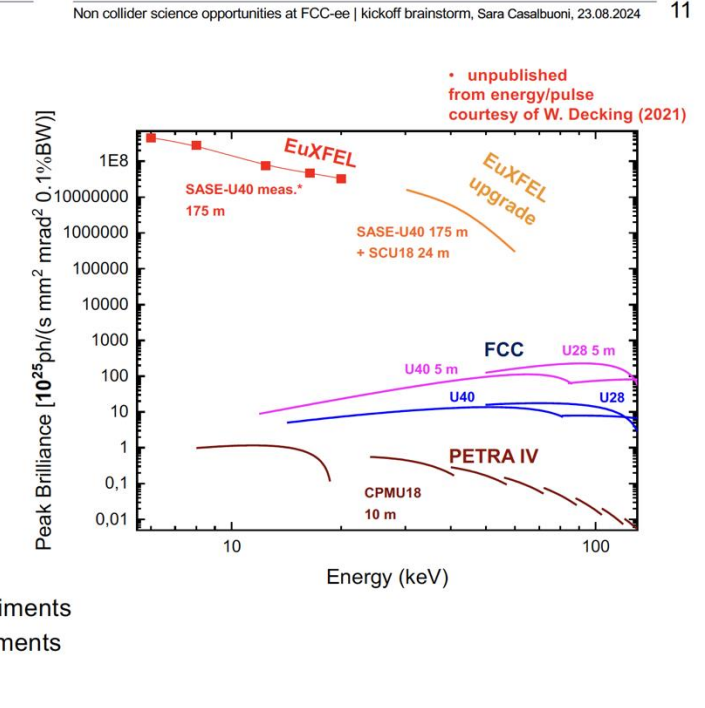
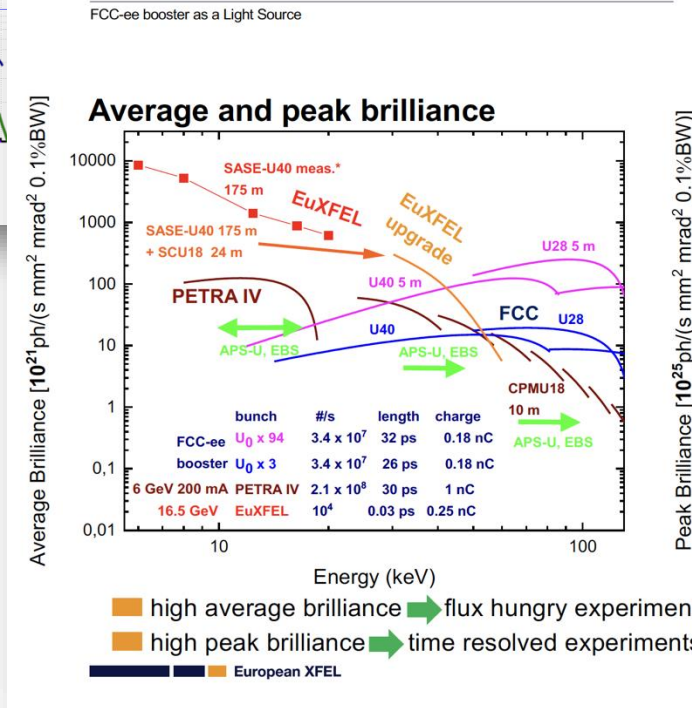
From August 2024 "Kick-off brainstorm" in Hamburg...

Compared to PETRA IV, at 50-100 keV the FCC-ee booster could produce:

- a fraction of coherent X-rays larger by one order of magnitude
- an average brilliance larger by up to two orders of magnitude
- a peak brilliance larger by up to four orders of magnitudes

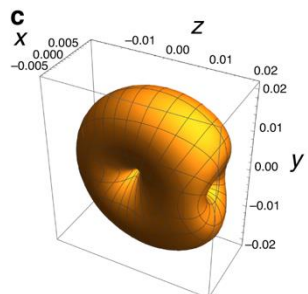
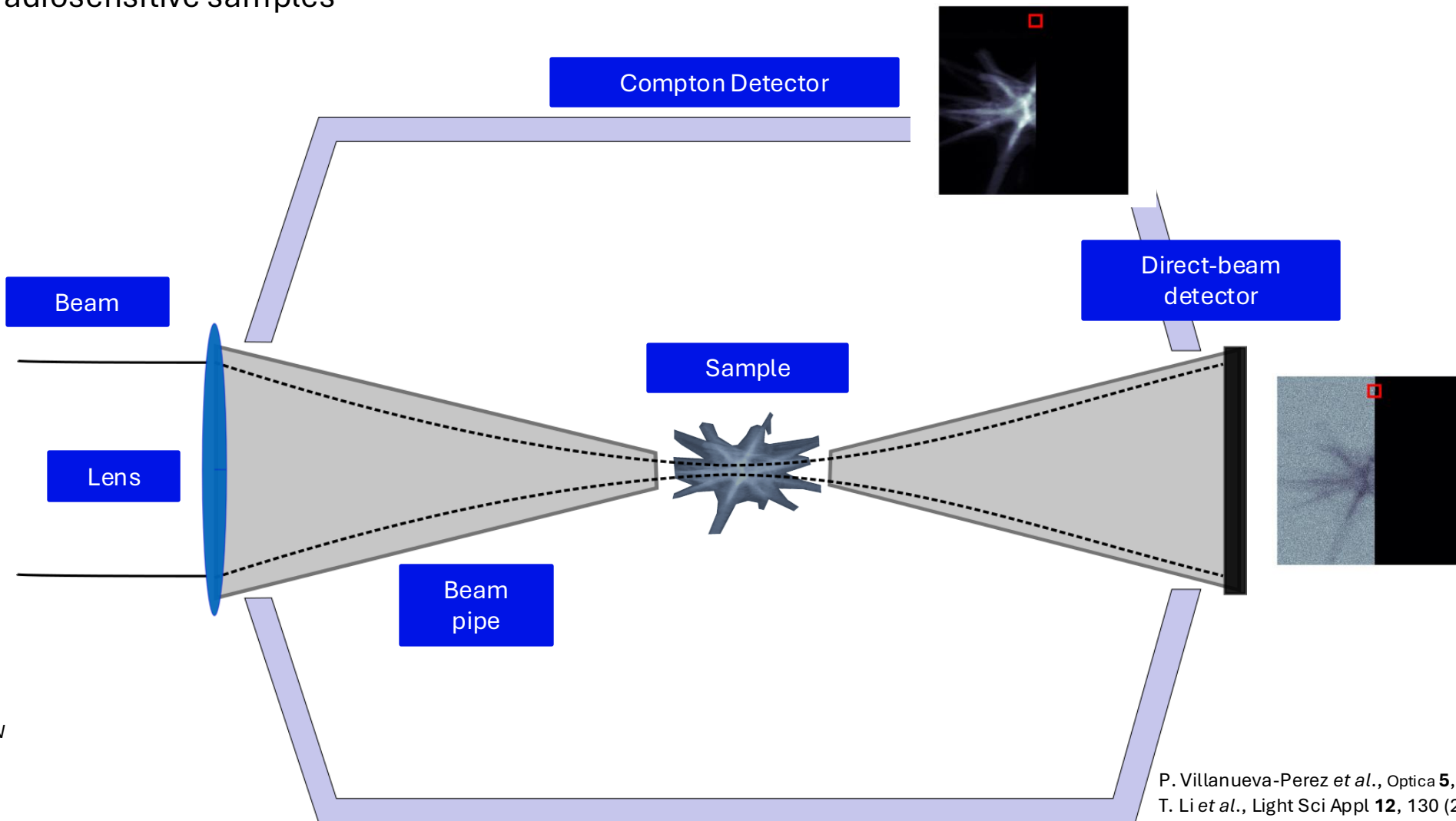
FCC-ee might boost imaging to unprecedented levels:

- Exceptional peak-brilliance and coherent fraction will enable high-energy time-resolved ptychographic imaging (larger samples, heavier materials, *in-situ/operando*)
- Exceptional average brilliance will push dynamic imaging beyond all currently achievable capabilities and eventually make scanning Compton X-ray Microscopy a valuable tool

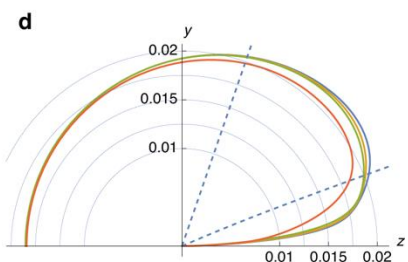


Scanning Compton X-ray microscopy (SCXM)

Currently neglected **Compton** interactions can lead to the highest achievable resolution when imaging biomedical and radiosensitive samples



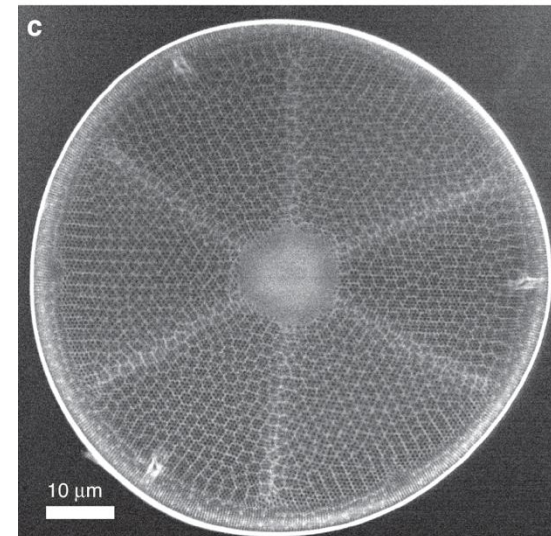
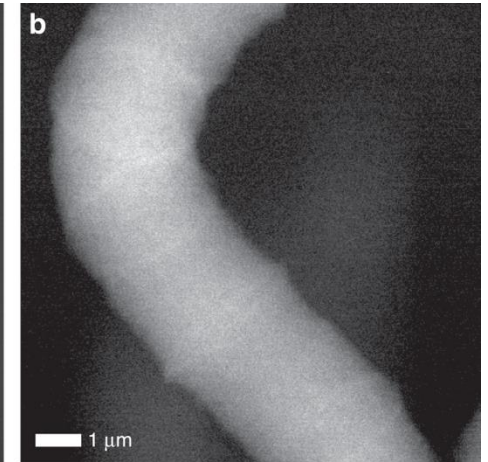
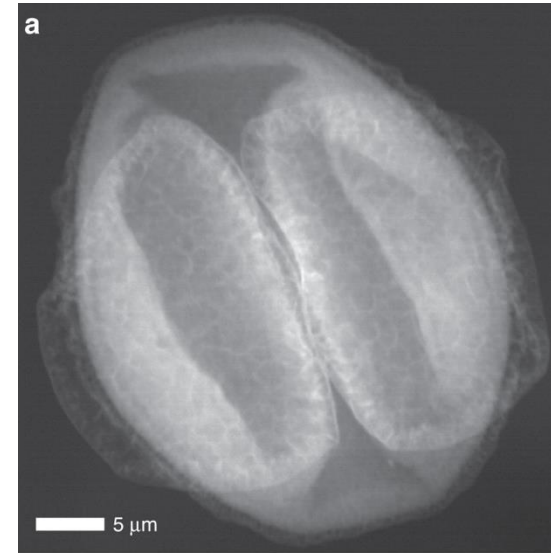
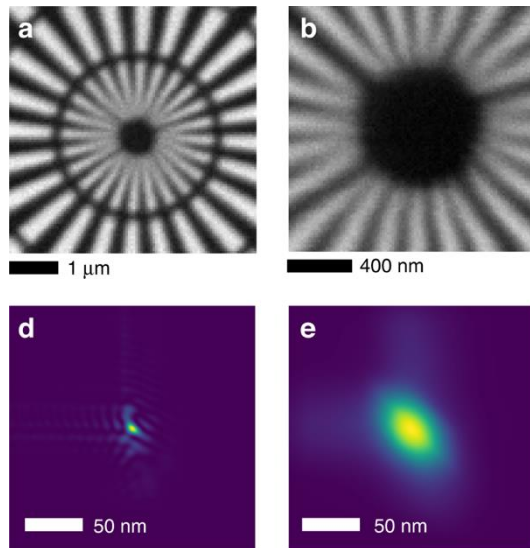
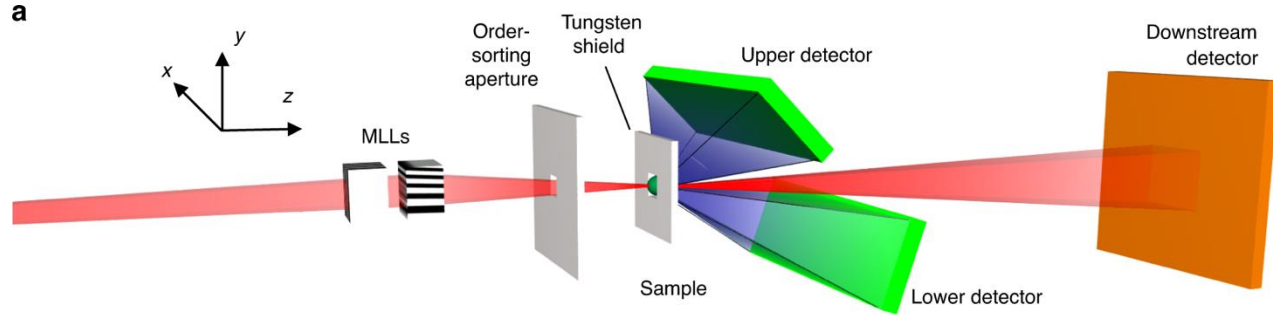
Differential cross section of carbon in units of $\text{cm}^2/\text{g}/\text{solid angle}$ at 60 keV photon energy



Slices of the differential cross sections in the same units of C (blue), N (yellow), O (green), and Si (orange).

P. Villanueva-Perez et al., *Optica* **5**, 450-457 (2018)
 T. Li et al., *Light Sci Appl* **12**, 130 (2023)

Scanning Compton X-ray microscopy (SCXM)



POC measurements on Petra II (P07)

- Resolution around 70-100 nm
- Overall performance limited by brilliance...

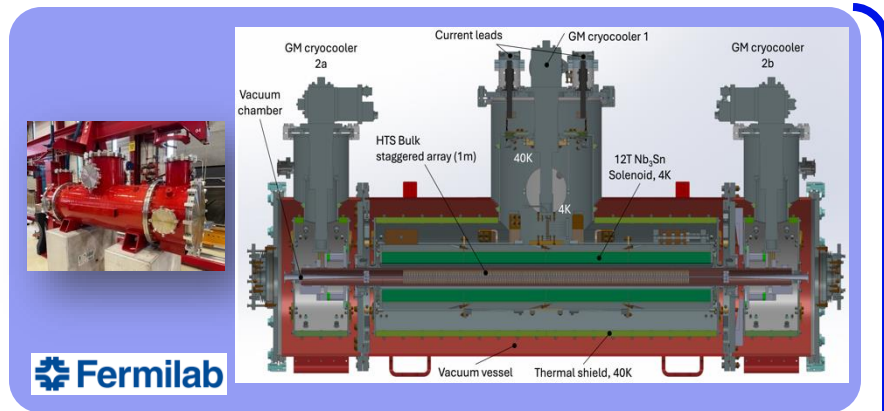
→ FCC-booster optimal source for SCXM

P. Villanueva-Perez, et al., *Opt. Lett.* **46**, 1920-1923 (2021)
 T. Li et al., *Light Sci Appl* **12**, 130 (2023)

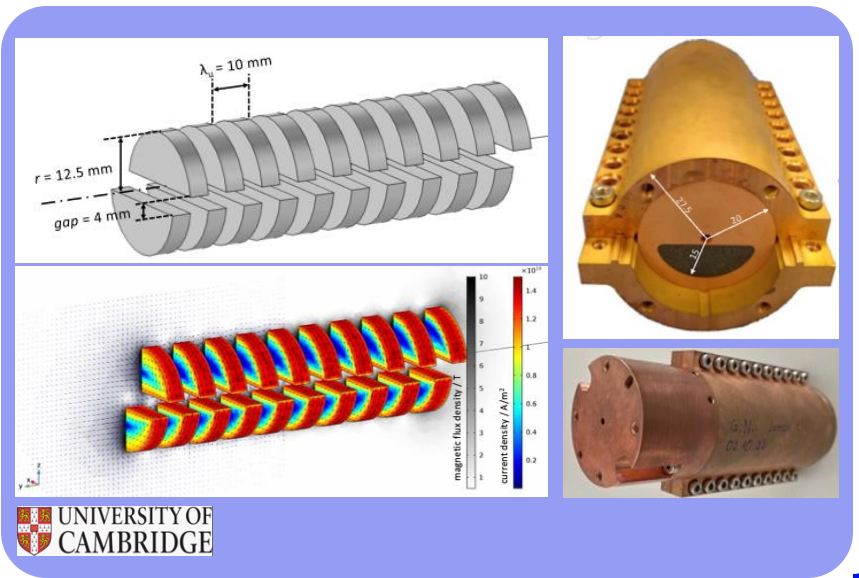
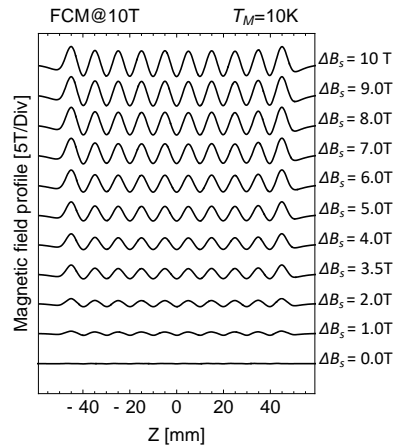
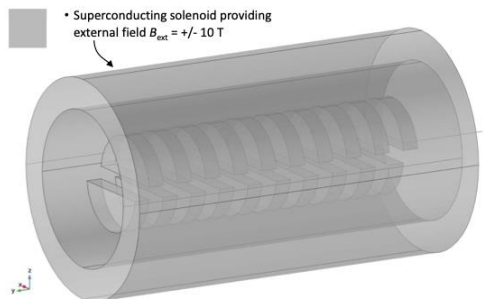
I-TOMCAT source: HTSU10 undulator



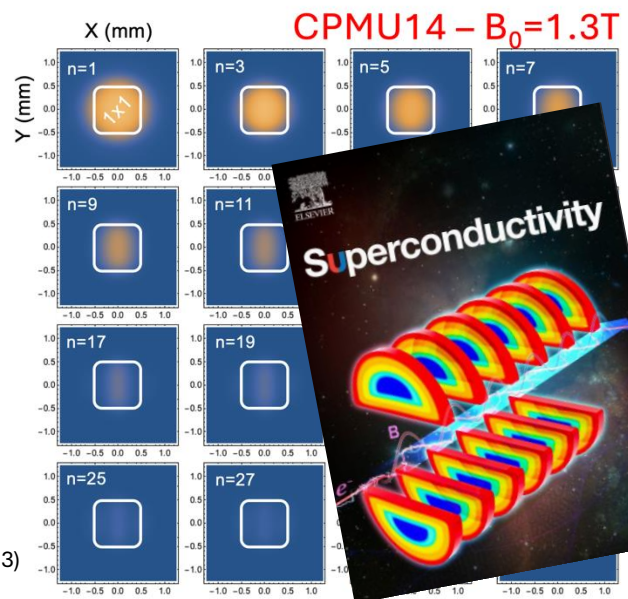
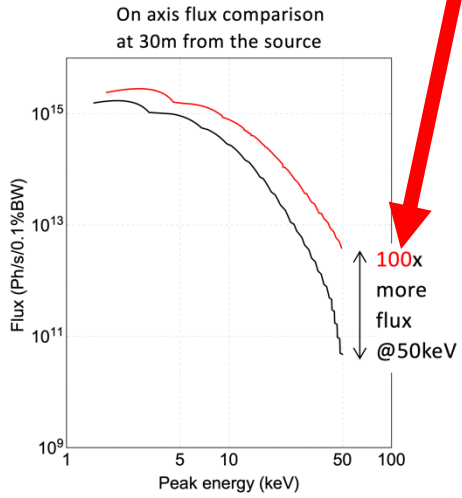
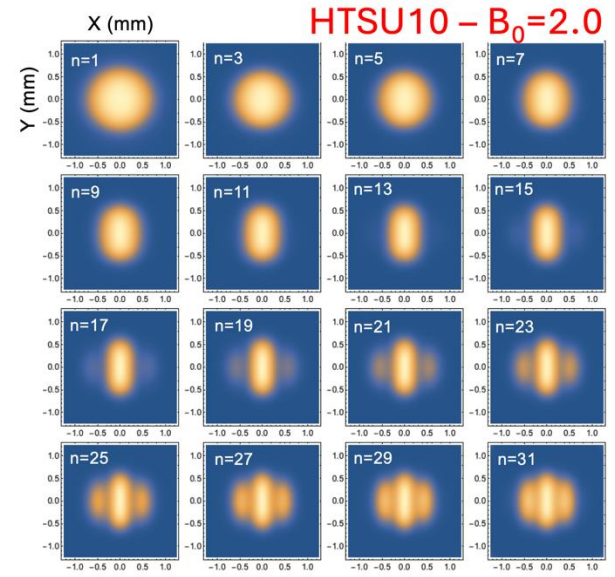
GdBCO by Nippon Steel – Design for 4.5 mm fix gap and 1.8T



Fermilab



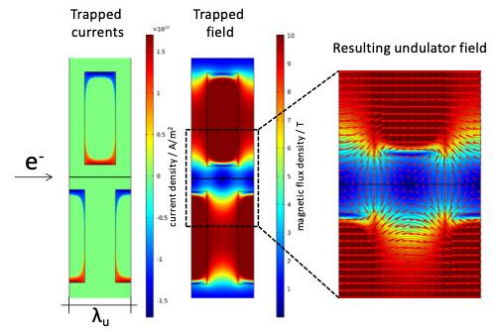
UNIVERSITY OF CAMBRIDGE



In-house development by M. Calvi

THE METER LONG PROTOTYPE

- Active length : 1.0 m
- Total length : < 2m
- period length : 10.5 mm
- magnetic gap : 4.5 mm
- B₀ ~ 1.8 T
- Cryocoolers
- HTS Mag-temp 10K
- LTS temp 4.0K



K. Zhang, M. Calvi et al., Superconductor Science and Technology 36 (2023)

